Cisplatin induces cytoplasmic to nuclear translocation of nucleotide excision repair factors among spiral ganglion neurons

ARTICLE *in* HEARING RESEARCH · JUNE 2008

Impact Factor: 2.97 · DOI: 10.1016/j.heares.2008.01.013 · Source: PubMed

4 AUTHORS, INCLUDING:

O'neil W Guthrie
Northern Arizona University
13 PUBLICATIONS **159** CITATIONS
SEE PROFILE

C.D. Balaban
University of Pittsburgh
204 PUBLICATIONS **4,358** CITATIONS
SEE PROFILE

Available online at www.sciencedirect.com
ScienceDirect
Hearing Research 239 (2008) 79–91
Hearing Research
www.elsevier.com/locate/heares

Research paper

Cisplatin induces cytoplasmic to nuclear translocation of nucleotide excision repair factors among spiral ganglion neurons

O'neil W. Guthrie [a,b,d,*], Ha-Sheng Li-Korotky [a,b], John D. Durrant [a,b], Carey Balaban [a,b,c]

[a] Department of Communication Science and Disorders, University of Pittsburgh, Forbes Tower 4033, Pittsburgh, PA 15260, USA
[b] Department of Otolaryngology, University of Pittsburgh, 107 Eye and Ear Institute, 203 Lothrop Street, Pittsburgh, PA 15213, USA
[c] Department of Neurobiology, University of Pittsburgh, Pittsburgh, PA 15213, USA
[d] Department of Biology, Developmental, Cell and Molecular Biology Group, Duke University, French Family Science Center, Science Drive, Rm. 4337, P.O. Box 90338, Durham, NC 27708-0338, USA

Received 4 September 2007; received in revised form 7 January 2008; accepted 31 January 2008
Available online 8 February 2008

Abstract

Genomic DNA is a high-affinity target for the antineoplastic molecule cisplatin. Cell survival from cisplatin DNA damage is dependent on removal of cisplatin-DNA adducts by nucleotide excision repair (NER) pathways. The rate-limiting steps in the NER pathways are DNA damage identification and verification. These steps are accomplished by xeroderma pigmentosum complementation group C and A (XPC and XPA) and RNA polymerase II. Unlike RNA polymerase II, XPC and XPA have no known cellular function beyond DNA repair. Cisplatin is known to damage spiral ganglion neurons at the basal coil of the cochlea therefore it was posited that cisplatin may target their DNA and mobilize XPC and XPA. Female Fisher344 rats were given two, four day cycles of cisplatin (2 mg/kg) or saline, separated by a 10 day rest period. A $2 \times 3 \times 2$ factorial design, consisting of two treatment conditions (cisplatin and saline treatment), three survival times (5, 19 and 22 days) and two analysis methods (quantitative RT-PCR and immunohistochemistry) was employed to evaluate the expression and distribution of XPC and XPA. Quantitative RT-PCR revealed statistically significant differences in cochlear XPC and XPA mRNA levels after cisplatin treatment at all times except day 22 for XPA. Immunohistochemistry revealed that a proportion (~50%) of spiral ganglion neurons in control rats showed cytoplasmic expression of XPC and XPA. After cisplatin treatment, a similar proportion (~50%) of spiral ganglion neurons showed increased nuclear expression of XPC and XPA, which appears to represent translocation from the cytoplasm. Basal coil spiral ganglion neurons translocated XPC and XPA at later treatment cycles and with less magnitude than apical coil neurons after cisplatin treatment. Therefore, it is suggested that cisplatin treatment induces nuclear translocation of NER proteins among spiral ganglion neurons and that this nuclear translocation is less efficient at the base relative to the apex.

Abbreviations: ABC, avidin-biotinylated enzyme complex; ABR, auditory brainstem response; BSA, bovine serum albumin; cDNA, complementary DNA; ΔCt, change in thermocycle threshold; DAB, 3.3′-diaminobenzidine tetrahydrochloride; dATP, deoxyadenosine triphosphate; dCTP, deoxycytidine triphosphate; dGTP, deoxyguanosine triphosphate; dNTP, deoxynucleotide triphosphate; DP-gram, distortion product-gram; DPOAE, distortion product otoacoustic emissions; dUTP, deoxyuridine triphosphate; 1,2-d(ApG), *cis*-[$(H_3N)_2$Pt{d(pApG)}]; 1,2-d(GpG), *cis*-[$(H_3N)_2$Pt{d(pGpG)}]; 1,3-d(GpNpG), *cis*-[$(H_3N)_2$Pt{d(GpNpG)}]; ERCC1-XPF, excision repair cross-complementing factor 1- xeroderma pigmentosum complementation group F; f_1, primary frequency 1; f_2, primary frequency 2; GG-NER, global genomic nucleotide excision repair; GSH, glutathione; GST, GSH-*S*-transferase; IHC, immunohistochemistry; L_1, primary tone level 1; L_2, primary tone level 2; *N*, total animals within a group; *n*, total animals in both groups; nt, nucleotide; NER, nucleotide excision repair; OAE, otoacoustic emissions; PCR, polymerase chain reaction; PLP, periodate–lysine–paraformaldehyde; rRNA, ribosomal ribonucleic acid; ROS, reactive oxygen species; ROX, 6-carboxy-X-rhodamine; RT-PCR, reverse transcription polymerase chain reaction; ΔRn, change in emission spectra of a normalized reporter; SL, sensation level; SYBR, [2-[*N*-(3-dimethylaminopropyl)-*N*-propylamino]-4-[2,3-dihydro-3-methyl-(benzo-1,3-thiazol-2-yl)-methylidene]-1-phenyl-quinolinium]$^+$; Taq, Thermus aquaticus; TC-NER, transcription coupled nucleotide excision repair; TFIIH, transcription factor-IIH; UNG, uracil *N*-glycosylase; UV, ultraviolet; XP, xeroderma pigmentosum; XPA, xeroderma pigmentosum complementation group-A; XPC, xeroderma pigmentosum complementation group-C

* Corresponding author. Address: Department of Biology, Developmental, Cell and Molecular Biology Group, Duke University, French Family Science Center, Science Drive, Rm. 4337, P.O. Box 90338, Durham, NC 27708-0338, USA. Tel.: +1 919 681 3804; fax: +1 919 613 8177.
E-mail address: owg@duke.edu (O.W. Guthrie).

0378-5955/$ - see front matter © 2008 Elsevier B.V. All rights reserved.
doi:10.1016/j.heares.2008.01.013

Keywords: Nucleotide excision repair; Cisplatin; Spiral ganglion neurons; Xeroderma pigmentosum; Ototoxicity; DNA adduct

1. Introduction

Cisplatin is an effective antineoplastic agent with dose-limiting nephrotoxicity and ototoxicity. Previous studies indicate that cisplatin has multiple intracellular targets, but the major cytotoxic effect appears to result from DNA adduct formation (e.g. Fraval and Roberts, 1979; Pera et al., 1981; Reed et al., 1987). Because cisplatin binds preferentially and covalently to available thiol-bearing biomolecules in the cytoplasm, the availability of ubiquitous thiols such as glutathione (GSH) serves a major role in preventing cisplatin toxicity (Ishikawa and Ali-Osman, 1993; Kartalou and Essigmann, 2001). In fact, the endogenous antioxidant glutathione is regarded as a primary vehicle for cytoplasmic detoxification of cisplatin (Goto et al., 1999), probably by limiting the concentration of cisplatin available for DNA binding. The acute administration of a single high dose of cisplatin can lead to glutathione depletion in the cochlea (Ravi et al., 1995) which is accompanied by a significant increase in antioxidant enzyme responses and signs of lipid peroxidation (Clerici et al., 1996; Ravi et al., 1995). The turnover and cisplatin binding kinetics of intracellular thiols (e.g. glutathione) may be a factor in the reported differences in the cochlear distribution of platinated DNA from a single high dose (Thomas et al., 2006) versus multiple cycles of low doses (van Ruijven et al., 2005) of cisplatin.

This study is the first examination of molecular responses of proteins associated with repair of cisplatin-induced DNA lesions in the inner ear. It is well-known in cancer research that cisplatin forms adducts that distort the helical structure of DNA (Zastawny et al., 1993). These DNA adducts represent covalent bonds between cisplatin and the DNA bases, particularly the purines, guanine and adenine (Redon et al., 2003). There is a strong positive correlation between the accumulation of cisplatin-DNA adducts and neoplastic cell death (Fraval and Roberts, 1979; Reed et al., 1987). In fact, one cisplatin-DNA adduct per 100,000–500,000 nucleotides is enough to induce cytotoxicity (Pera et al., 1981). Although cisplatin-DNA adducts are widespread in the cochlea after systemic drug administration (van Ruijven et al., 2005; Thomas et al., 2006), cellular mechanisms of DNA repair have not been explored in the inner ear.

Nucleotide excision repair (NER) is the primary DNA repair pathway that removes cisplatin-DNA adducts from the genome and appears to confer cellular resistance to cisplatin toxicity. For example, cisplatin is exceptionally effective (99% cure rate) at killing testicular cancer cells (Giaccone, 2000), which are deficient in NER activity (Koberle et al., 1999). However, ovarian cancer and small cell lung cancers may initially respond to cisplatin treatment but later develop resistance that is correlated with increased NER activity (Dabholkar et al., 1994; Ferry et al., 2000; Giaccone, 2000; Selvakumaran et al., 2003). Suppression of NER activity also confers sensitivity to cisplatin damage (Wu et al., 2003). Finally, NER is the only known molecular mechanism by which cisplatin-DNA adducts can be repaired leading to cell survival (Welsh et al., 2004; Wu et al., 2003).

NER operates through two pathways that differ only in the way lesions are identified (Thoma and Vasquez, 2003; de Laat et al., 1999). The global genome-NER (GG-NER) pathway identifies DNA damage on genes that are not transcribed (Costa et al., 2003; de Laat et al., 1999). Recognition of lesions in the GG-NER pathway requires activation of the NER protein, xeroderma pigmentosum complementation group-C (XPC) and its conjugates (Boonstra et al., 2001; Chen et al., 2003). In fact, absence of XPC results in failure of only GG-NER (Costa et al., 2003; de Laat et al., 1999). XPC first identifies cisplatin-induced chemical and physical alterations to non-transcribed DNA (silent genes) and sequesters other NER protein-enzymes to the site of damage. For instance, XPC recruits helicases which open the DNA helix to prepare for docking of the NER protein xeroderma pigmentosum complementation group-A (XPA) (Riedl et al., 2003). XPA (32 kDa) is a zinc-finger DNA binding protein with high-affinity for cisplatin-DNA adducts. It verifies that a lesion is significant and coordinates repair activities (Boonstra et al., 2001; de Laat et al., 1999). Beyond NER, XPA has no known cellular function (de Laat et al., 1999; Thoma and Vasquez, 2003). In fact inhibition of XPA renders tumor cells unable to complete NER (Koberle et al., 1999; Rosenberg et al., 2001) and testicular tumor cells that are highly sensitive to cisplatin are deficient in XPA expression (Welsh et al., 2004). Once XPA verifies the lesion, DNA repair continues with exonucleation of the damaged oligonucleotides (~30 nt) and polymerization of a new oligoneucleotide strand.

The transcription coupled NER (TC-NER) pathway repairs DNA damage on transcribed (active) genes (de Laat et al., 1999). It is initiated by RNA polymerase II during transcription. Here, RNA polymerase II stalls at the site of lesion, which allows for quick identification and titration of NER enzymes (Tornaletti et al., 2003). Activation of XPA is essential to both NER pathways (de Laat et al., 1999) because, suppression of XPA results in defective GG-NER and TC-NER (Boonstra et al., 2001; Rosenberg et al., 2001). The rate-limiting steps for both NER pathways are lesion identification and verification (Thoma and Vasquez, 2003). In TC-NER these steps are accomplished by RNA polymerase II and XPA while GG-NER relies on XPC and XPA. Unlike RNA polymerase II, XPC and XPA have no known cellular function beyond DNA repair (Costa et al., 2003). XPC is a marker for only

GG-NER while XPA is a marker for both TC-NER and GG-NER (de Laat et al., 1999; Thoma and Vasquez, 2003). Both GG-NER and TC-NER are needed in order to defend the genome from toxic insults.

Recent studies have shown that different schedules of systemic cisplatin treatment result in cellular accumulation of platinated DNA adducts in the cochlea (van Ruijven et al., 2005; Thomas et al., 2006). Furthermore, cisplatin exposure is associated with the loss of a proportion of human spiral ganglion neurons (Cheng et al., 2001; Hoistad et al., 1998; Strauss et al., 1983). The present study provides the first demonstration that sub-cytotoxic cisplatin treatment cycles mobilize the rate-limiting NER proteins, XPC and XPA among spiral ganglion neurons. These findings may help elucidate mechanisms underlying damage to a proportion of human spiral ganglion neurons after cisplatin treatment (Cheng et al., 2001; Hoistad et al., 1998; Strauss et al., 1983).

2. Materials and methods

2.1. Animals

This study used a protocol established by Minami et al. (2004) that utilizes multiple cycles of relatively low cisplatin doses in female Fischer344 rats. This protocol was selected because it provides an opportunity to study responses to repeated cycles of exposure that are encountered in chemotherapy. Sixty female Fischer344 rats (140–160 g) were acquired from Charles River Laboratories, Malvern, PA, USA. The animals had free access to both food and water and were weighed daily. They were housed in a room (23 ± 2 °C) on a 12-h light/dark cycle. All experimental protocols were performed according to National Institute of Health (NIH) guidelines and were approved by the Institutional Animal Care and Use Committee (IACUC) at the University of Pittsburgh, Pittsburgh, PA. The IACUC approval process certifies that all protocols are in compliance with the United States Department of Agriculture and NIH guidelines for ethical treatment of animals and that all attempts were made to minimize both animal use and suffering.

2.2. Drug administration

In this study, repeated cycles of low dose cisplatin (Minami et al., 2004) were employed to test the hypothesis that NER responses would differ between exposure cycles. Protocols using repeated cycles of relatively low dose cisplatin treatment (cycles of 4 days at 2 mg/kg, i.p., per day) have been reported to deplete antioxidant responses in the Fischer344 rat cochlea (Minami et al., 2004) and produce cisplatin-DNA adducts in the guinea pig cochlea (van Ruijven et al., 2005). A $2 \times 3 \times 2$ factorial design, consisting of two treatment conditions (cisplatin and saline treatment), three survival times and two analysis methods (quantitative RT-PCR and immunohistochemistry) was employed. Cisplatin was supplied by Sigma (St. Louis, MO) and dissolved in sterile physiological saline (pH 7.4) to a concentration of 0.1 mg/ml (Minami et al., 2004; van Ruijven et al., 2005). This stock solution was shielded from light and stored at 5° C. The rats were treated with two cycles of cisplatin (Minami et al., 2004), each cycle consisting of 4 days of treatment (1 mg/kg, i.p., twice daily) separated by 10 days of rest. Each animal received daily hydration therapy consisting of 10 ml of saline administered subcutaneously. Survival times were 24 h after each treatment cycle (days 5 and 19) and 4 days (recovery period) after the second treatment cycle (day 22). A total of 30 animals were treated with cisplatin, 10 were sacrificed at each of the three survival times for analyses. The cisplatin treated animals showed a 10% average weight loss. Thirty rats served as control by receiving sterile physiological saline (vehicle) instead of cisplatin. Table 1 summarizes the research design.

2.3. Auditory brainstem response and otoacoustic emissions

In order to monitor cochlear integrity during cisplatin treatment cycles, the visual detection level of auditory brainstem response (ABR) and magnitude of otoacoustic emissions (OAE) were recorded. Similar recordings were obtained from the saline treated group which allowed for derivation of ABR threshold shifts in dB SL (sensation level) and OAE amplitude shifts. The ABR was recorded under general anesthesia (ketamine 75 mg/kg, i.p. and xylazine 8 mg/kg, i.p.; Minami et al., 2004). Each animal was placed on a heating pad maintained at $38° \pm 5$ °C. All recordings were performed in a sound isolation chamber. Five subdermal needle electrodes were used for two-channel recordings. Two electrodes (positive) were placed on the vertex, one was placed below the right and left mastoids (negatives) and one electrode (ground) was placed in the dorsum close to the tail. The stimuli were synthesized digitally and presented through an insert earphone (Etymotic Research ER-3A). The transducer was coupled acoustically to the ear with a pediatric probe tip. The intensity of the acoustic stimuli was expressed in decibel sound pressure level (dB SPL). The animals were presented with a stimulus intensity series that was initially presented nominally at 90 dB SPL and progressively lowered in 10 dB steps. Threshold was defined as the lowest level that elicited a repeatable waveform with identifiable waves I and II. The stimulus frequencies were 4, 8 and 16 kHz tone pips (1 ms rise-fall time, 10 ms plateau). Each ABR recording represented the average of individually amplified and filtered responses. ABR thresholds from the control group were subtracted from that of the cisplatin treated group to determine thresholds in SL. The threshold shifts observed were taken as estimates of hearing loss, analogous to conventional audiometry.

The cubic $2f_1$–f_2 distortion product otoacoustic emission (DPOAE) was recorded using two primaries, f_1 and f_2 (ratio: $f_2/f_1 = 1.22$). The primary tone levels (L) for f_1 and

Table 1
Study design

Group	Days 1–4 (cycle 1)	Day 5	Days 5–14	Day 15–18 (cycle 2)	Day 19	Day 19–21	Day 22
$n = 60$	$n = 60$	$n = 60$–20	$n = 40$	$n = 40$	$n = 40$–20	$n = 20$	$n = 20$–20
Experimental $N = 30$	Cisplatin treatment $N = 30$	ABR and OAE ($N = 10$) euthanasia for: 1. IHC, $N = 5$ 2. PCR, $N = 5$	Rest period for the 20 remaining rats	Cisplatin treatment $N = 20$	ABR and OAE($N = 10$) euthanasia for: 1. IHC, $N = 5$ 2. PCR, $N = 5$	Rest period for the 10 remaining rats	ABR and OAE($N = 10$) euthanasia for: 1. IHC, $N = 5$ 2. PCR, $N = 5$
Control $N = 30$	Saline treatment $N = 30$	ABR and OAE($N = 10$) euthanasia for: 1. IHC, $N = 5$ 2. PCR, $N = 5$	Rest period for the 20 remaining rats	Saline treatment $N = 20$	ABR and OAE ($N = 10$) euthanasia for: 1. IHC, $N = 5$ 2. PCR, $N = 5$	Rest period for the 10 remaining rats	ABR and OAE ($N = 10$) euthanasia for: 1. IHC, $N = 5$ 2. PCR, $N = 5$

f_2 were $L_1/L_2 = 60/50$ dB SPL. DP-grams (the function of DPOAE level on increasing stimulus frequency) were recorded with a resolution of four points per octave regarding f_2. DPOAE amplitudes from the cisplatin treated group were subtracted from that of the control group to derive amplitude shifts. Both ABR and DPOAE acquisition, stimulus presentation, equipment control and data management were facilitated by instrumentation and software from Intelligent Hearing System, Miami, FL.

3. Reverse-transcription real-time quantitative PCR

3.1. Animals and tissue preparation

Fifteen Fischer344 rats from each group were sacrificed by decapitation following pentobarbital anesthesia (100 mg/kg, i.p.). Inner ear tissues (organ of Corti, modiolus, lateral wall and spiral ganglia) were rapidly dissected from the otic capsule under a stereomicroscope in ice-cold PBS (pH 7.4), rapidly frozen on dry ice and stored at −80 °C for later processing. Kidney and liver tissues also were harvested and processed in a similar manner.

3.2. Total RNA extraction

Dissected cochlear tissues were thawed, pooled and homogenized in TRIzol™ (Invitrogen, Carlsbad, CA, USA) reagent (1 ml per 50–100 mg of tissue). Chloroform was then added and the mixture was centrifuged in order to separate the RNA phase from the DNA phase. The RNA phase was used for RNA precipitation using isopropyl alcohol. The RNA samples were rinsed with 75% ethanol and solubilized with RNase-free water. The RNA was then digested with DNase I (Ambion, Inc., Austin, TX, USA) to remove DNA contamination.

3.3. Reverse transcription of RNA

The DNA-free RNA was converted to complementary DNA (cDNA) through reverse transcription. The reverse transcription reaction included 10 μl of 10 × PCR Taq Gold Buffer II (Applied Biosystems Inc., Foster City, CA), 30 μl of 25 mM $MgCl_2$, 4 μl of 25 mM of each dNTP, 5 μl of 100 μM of random primer (GIBCO), 2 μl of RNasin (40 units; Applied Biosystems Inc.), 1.25 μl of SuperScript II (250 units; GIBCO) and 200 ng of DNA-free total RNA. The reaction mixture was incubated at 25 °C for 10 min, 48 °C for 30 min, and 95 °C for 5 min in a 9600 thermocycler (Applied Biosystems Inc.).

3.4. Real-time quantitative PCR

SYBR green chemistry (Applied Biosystems Inc.) was used for real-time quantitative PCR. The reaction included 5 μL of 10 × SYBR green PCR Buffer, 6 μL of 25 mM $MgCl_2$, 4 μL of each dNTPs (blended with 2.5 mM dATP, dGTP and dCTP, and 5 mM dUTP), 2.5 μL of each gene-specific primer (5 μM), 0.5 μL of AmpErase UNG (0.5 unit), 0.25 μl of AmpliTaq Gold (1.25 units) and 5 μL of cDNA in a final volume of 50 μL. The conditions for the SYBR green PCR were as follows: 50 °C for 2 min, 95 °C for 12 min, and 40 cycles at 95 °C for 15 s, and 60 °C for 1 min in an ABI PRISM 7700 Sequence Detection system (Applied Biosystems Inc.). Gene-specific primers for the target molecules are shown in Table 2.

3.5. Data analysis

Instrument control, automated data collection, and data analysis were accomplished using the 7700 Sequence Detec-

Table 2
Gene-specific primers for PCR of XPC, XPA and 18S rRNA genes

XPC (accession no. XM_232194)	
Forward primer	5′-CAGCCTTTGCCCACCTCCA-3′
Reverse primer	5′-TCCACGACAATACCCAAGGAC-3′
XPA (accession no. XM_216403)	
Forward primer	5′-AAGAAGAACCCTCGCCATTCA-3′
Reverse primer	5′-TTCAAGAGCCCGCTTTACAAC-3′
Rat 18S rRNA (accession no. X01117)	
Forward primer	5′-AAGCCATGCATGTCTAAGTACGCA-3′
Reverse primer	5′-AAGTAGGAGAGGAGCGAGCGACCA-3′

tion Software (Applied Biosystems Inc.). For each assay, logarithmic amplification plots were constructed based on cDNA copy number of a target gene normalized to the ROX internal passive reference (log ΔRn) versus cycle number. The cycle number at which the signal crossed the mid-linear portion of the log ΔRn-cycle function was defined as the cycle threshold (Ct) (Schmittgen et al., 2000). The level of gene expression was calculated using $2^{-\Delta Ct}$ (Livak and Schmittgen, 2001). The ΔCt represents the Ct of the target gene normalized to the rat endogenous 18S rRNA ($\Delta Ct = Ct_{Target} - Ct_{18S\ rRNA}$). The $2^{-\Delta Ct}$ calculation satisfies assumptions for the use of parametric statistics such as *t*-test and ANOVA (Livak and Schmittgen, 2001).

4. Immunohistochemistry

4.1. Animals and tissue preparation

Fifteen Fischer344 rats from each group were sacrificed with pentobarbital anesthesia (100 mg/kg, i.p.) and perfused transcardially with phosphate-buffered saline (PBS; 0.9% NaCl in 50 mM phosphate buffer, pH 7.3), followed by periodate–lysine–paraformaldehyde (PLP) fixative (McLean and Nakane, 1974). The heads were removed, skinned and then post-fixed in 4% paraformaldehyde for at least 24 h at 22 °C. Decalcification of the heads occurred in 10% formic acid then neutralized overnight in 5% sodium sulfite by standard methods prior to trimming and paraffin embedding. Paraffin embedded sections were cut with a microtome at 8 μm and mounted on subbed slides. The sections were then stored at 22 °C prior to immunohistochemistry.

4.2. Immunohistochemical procedure

Tissue sections were de-paraffinized and treated for 10 min with 30% H_2O_2 in dH_2O and then rinsed thoroughly with dH_2O. They were then heated for 20 min at 90–98 °C in a low pH (0.80–3.06) sodium citrate–citric acid buffer (antigen retrieval) and rinsed thoroughly with PBS. Afterwards, the sections were pre-treated with a blocking solution of normal horse or goat serum, 10% Triton X-100 and 2% bovine serum albumin (BSA; Sigma, St. Louis, MO, USA) in PBS for 1 h. The primary antibodies were diluted in the blocking solution at a 1:200 concentration. The primary antibodies were anti-XPC (sc-22535) and anti-XPA (sc-853) (Santa Cruz Biotechnology, Inc.). Both negative (primary antibody was omitted) and preadsorbed controls were used. The XPA antibody was preadsorbed at room temperature for 4 h with an excess (1 μg peptide per 10 μL antibody) 40 kDa tagged fusion protein that corresponds to amino acids 1–273 of human XPA (dialyzed Santa Cruz product sc-4331 WB). The XPC blocking peptide (1 μg peptide per 10 μL antibody for 4 h at room temperature) was the oligopeptide antigen (Santa Cruz product sc-22535) for raising the anti-XPC. After 24 h incubation at 22 °C with the primary anti-bodies the sections were rinsed with PBS. They were then treated with biotinylated anti-goat or anti-rabbit secondary antibodies (Vector Laboratories, Temecula, CA, USA; diluted 1:500 in PBS + 2% BSA) for 1 h at 22 °C. The sections were then rinsed in PBS, incubated with Vectastain ABC reagent (Vector Laboratories) for 1 h, rinsed again with PBS and then treated with a solution of Trizma pre-set crystals (1.58 g; Sigma). The sections were washed in PBS and then stained for 10 min with 3,3′-diaminobenzidine tetrahydrochloride (DAB staining). These sections were then dehydrated by increasing concentrations of ethanol, treated with xylene and cover-slipped with Permount.

4.3. Data analysis

Serial horizontal sectioning through the otic capsule produced para-mid-modiolar cochlear sections. Spiral ganglion cells at the base, middle and apical turns of the cochlea were counted for cisplatin and saline treated animals after days 5, 19 and 22. The proportion of spiral ganglion cells showing cytoplasmic, nuclear and no-immunoreactivity was determined from each cochlear turn on each day for each animal ($N = 30$). Analysis of variance (ANOVA) followed by post-hoc multiple range tests were used to determine significant differences between saline and cisplatin treated groups and between days.

5. Results

5.1. Auditory brainstem response and otoacoustic emissions

The auditory brainstem response (ABR) and otoacoustic emission (OAE) data showed slight evidence of cochlear damage in the cisplatin-treated groups at the three survival times. The mean ABR threshold shift did not exceed 14 dB (see Fig. 1A). Mixed model analysis of variance (frequency (4 kHz, 8 kHz and 16 kHz, within groups factor) × treatment (control versus cisplatin, between groups factor) × day (day 5, day 19 or day 22, between groups data)) revealed significant main effects of treatment ($F(1,50) = 9.57$, $p < 0.01$) and day ($F(2,50) = 5.305$, $p < 0.01$) and frequency ($F(2,100) = 603.5$, $p < 0.001$) and a significant frequency × treatment interaction effect $F(2,100) = 4.51$, $p < 0.01$). The factors underlying these differences were clarified by separate analyses (ANOVA followed by Fisher's least significant differences tests) of the data for each frequency on each day. There were significant threshold shifts (LSD test differences between cisplatin and control groups) on day 5 at 8 kHz ($p < 0.05$), on day 19 at 16 kHz ($p < 0.05$) and 8 kHz, and significant shifts at 16 kHz ($p < 0.05$) and 8 kHz ($p < 0.05$) on day 22. The threshold shift on day 22 at 4 kHz was marginally significant ($F(1,17) = 4.37$, $p = 0.052$). The mean OAE amplitude shifts were at worst only 6 dB and did not differ statistically from the respective control groups (see Fig. 1B). Microscopic examination of the cochlea in hematoxylin-eosin

stained sections showed no evidence of either hair cell or spiral ganglion cell loss after cisplatin treatment at these short survival times. Hence, cochlear cells appear to have been viable when tissues were harvested to evaluate gene and protein expression responses to cisplatin treatment.

5.2. Real-time quantitative RT-PCR

Real-time quantitative RT-PCR showed that XPC mRNA expression increased very modestly (less than 2-fold) in the inner ear tissue samples after each cisplatin treatment cycle. By contrast, there was no change in XPA or XPC mRNA expression in the liver and kidney samples from the corresponding treatment groups (data not shown). Fig. 2A, shows the level of expression of XPC mRNA after the first (day 5) and second (day 19) treatment cycles and 4 days after the end of the second treatment cycle (day 22). The level of XPC mRNA expression was greater after cisplatin treatment on all days compared to saline treatment (ANOVA, main effect of treatment, $F(1,6) = 27.5$, $p < 0.01$). XPC mRNA expression was elevated significantly in the cisplatin relative to the saline treated groups for day 5 ($t(10) = -3.164$, $p < .05$), day 19 ($t(10) = -3.817$, $p < .01$) and day 22 ($t(10) = -5.622$, $p < .001$). However, ANOVA revealed that XPC gene expression did not significantly change across days during saline ($F(2,10) = 1.763$, $p > .05$) or cisplatin ($F(2,10) = .503$, $p > .05$) treatment. Fig. 2B shows the level of expression of XPA after the first (day 5) and second (day 19) treatment cycles and 4 days after the last treatment cycle (day 22). The level of XPA mRNA was also greater after cisplatin treatment relative to saline treatment (ANOVA, main effect of treatment, $F(1,6) = 13.9$, $p < 0.01$), but independent samples t-tests showed that mean XPA mRNA levels were elevated in the cisplatin group (relative to saline control) only for day 5 ($t(10) = -2.706$, $p < .05$) and day 19 ($t(10) = -6.899$, $p < .001$). There was no difference in the XPA mRNA level between cisplatin and saline treated groups on day 22.

One unexpected finding in the saline control group was that the XPA mRNA level was significantly lower on day 19 than on either day 5 or day 22 (ANOVA main effect and Fisher least significant differences tests, $p < 0.05$), with no significant difference between days 5 and 22. However, there was no significant difference in XPA mRNA expression in the cisplatin group across days. The combined real-time quantitative PCR data suggest that the cisplatin treatment cycles produced a very modest (less than 2-fold) elevation of XPC and XPA gene expression without inducing cellular degeneration.

5.3. Immunoreactivity

The XPC- and XPA-immunopositive spiral ganglion cells displayed either a cytoplasmic or a nuclear pattern of expression. Immunostaining was absent in preadsorbed control sections. Fig. 3 shows high magnification photomicrographs of these intracellular patterns of XPC immunoreactivity in spiral ganglion neurons. The cytoplasmic pattern of staining was a granular to homogeneous appearance of reaction product within the soma, with a prominent unstained nucleus. This pattern of staining is consistent with the presence of translated proteins within the cytoplasm. The nuclear pattern of staining was defined by a dense accumulation of immunoreactivity in the nucleus, often with residual staining in the cytoplasm. This latter pattern is consistent with activation of NER proteinenzymes to bind with damaged DNA in the nucleus (Rademakers et al., 2003; Moné et al., 2004; Politi et al., 2005; Wu et al., 2007).

There was a marked and highly consistent change in the intracellular staining patterns for XPC and XPA after

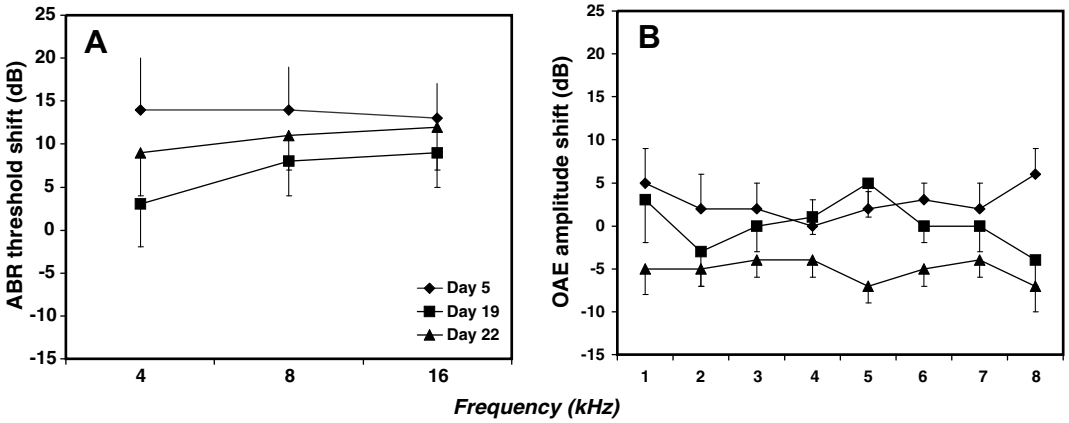

Fig. 1. ABR threshold shifts and OAE amplitude shifts after day 5 ($n = 20$), day 19 ($n = 20$) and day 22 ($n = 20$) of cisplatin ($n = 30$) or saline ($n = 30$) treatment. (A) ABR threshold shifts were assessed at 4, 8 and 16 kHz after cisplatin treatment. Day 5 revealed the highest threshold shifts followed by day 22 then day 19. Note that the worst threshold shift is only 14 dB, a mild shift in ABR sensitivity due to cisplatin treatment. (B) OAE amplitude shifts were assessed between 1 and 8 kHz after cisplatin treatment. Day 5 revealed the highest amplitude shifts followed by day 19 then day 22. Note that the worst amplitude shift is only 6 dB which suggest a slight shift in OAE sensitivity due to cisplatin treatment. The combined ABR and OAE results suggest that cochlear function was preserved after cisplatin treatment. ABR threshold shifts and OAE amplitude shifts are expressed as mean values ± SE.

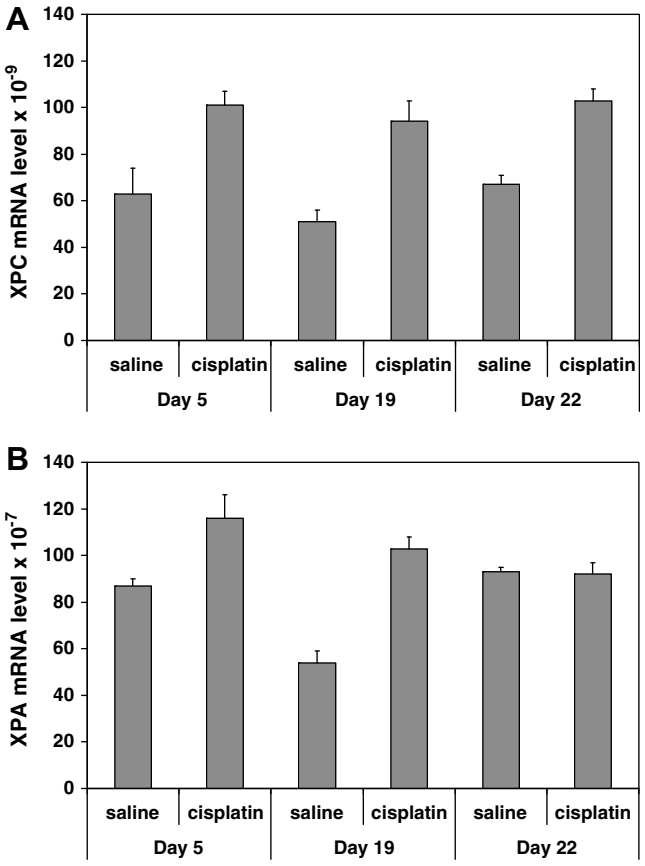

Fig. 2. Cisplatin treatment slightly increases cochlear XPC and XPA mRNA levels ($2^{-\Delta Ct}$: y-axis). (A) XPC mRNA level for saline ($n = 15$) and cisplatin ($n = 15$) treated groups after days 5 ($n = 5$), 19 ($n = 5$) and 22 ($n = 5$). (B) XPA mRNA level for saline ($n = 15$) and cisplatin ($n = 15$) treated groups after days 5 ($n = 5$), 19 ($n = 5$) and 22 ($n = 5$). Each bar represents mean ± SE for triplicate runs.

cisplatin treatment. These staining features are shown in photomicrographs in Fig. 4 and graphically in Figs. 5–7. Although there were changes in the proportion of spiral ganglion cells showing cytoplasmic and nuclear staining for each protein, the temporal and spatial patterns of changes differed between XPC and XPA. The results of analysis of variance of these patterns are summarized in Tables 3 and 4.

The initial significant change in the intracellular distribution of XPC occurred throughout the turns of the cochlea after the first cycle of cisplatin treatment (day 5). Although there was no significant difference in the total proportion of spiral ganglion cells expressing XPC (Fig. 7), there was a significant increase in the proportion of ganglion cells showing a nuclear distribution of XPC (Figs. 4A, 5). The proportion of ganglion cells showing nuclear XPC immunoreactivity was elevated significantly in cisplatin-treated rats ($F(1,8) = 26.65$, $p < 0.01$), with significant elevations in all cochlear turns ($p < 0.05$ relative to respective control rats). However, the proportion of ganglion cells showing a cytoplasmic distribution of XPC on day 5 was more variable and did not differ between treatment groups. After the second cycle of cisplatin treatment (day 19), there was no significant effect of cisplatin treatment on either the proportion of ganglion cells showing nuclear XPC expression or the proportion showing cytoplasmic XPC expression (Fig. 5). By day 22, the proportion of XPC-positive ganglion cells was elevated significantly in the cisplatin treated group ($F(1,8) = 9.70$, $p < 0.05$), reflecting an increase in the proportion of ganglion cells expressing cytoplasmic XPC ($F(1,8) = 5.92$, $p < 0.05$). The predominant cytoplasmic distribution of XPC immunoreactivity on days 19 and 22 are shown in Fig. 4B and C, respectively. Hence, the increase in cochlear XPC mRNA on day 5 in the cisplatin-treated group (Fig. 2A) appears to be associated temporally with a translocation of XPC into the nuclei of the ganglion cells.

The intracellular distribution of XPA showed clear evidence of a nuclear translocation response to both cycles of cisplatin treatment (Figs. 4 and 6). Cisplatin did not affect the overall proportion of spiral ganglion cells that expressed XPA on days 5 or 19 (Fig. 7). However, there was a highly significant increase in proportion of cells in the cisplatin-treated group with nuclear XPA immunoreactivity on both day 5 (Fig. 6, main effect of treatment: $F(1,8) = 6.17$, $p < 0.05$) and day 19 (Fig. 6, main effect of treatment: $F(1,8) = 11.63$, $p < 0.01$), accompanied by significant decreases in the proportion of cells with cytoplasmic XPA expression (day 5: treatment main effect $F(1,8) = 10.31$, $p < 0.05$; day 19: treatment main effect $F(1,8) = 28.2$, $p < 0.01$). The changes in nuclear expression were significant only in the middle and apical turns of the cochlea on day 5, but were also significant in the basal turn on day 19. No significant effects were found in the pattern of XPA immunoreactivity on day 22. Fig. 4D–E illustrate the increased proportion of spiral ganglion cells with nuclear XPA immunoreactivity on days 5 and 19, respectively; the return of a control pattern of staining is shown in Fig. 4F.

6. Discussion

This study provides the first documentation of NER protein responses of inner ear ganglion cells to systemic cisplatin exposure. Both XPC and XPA showed evidence of translocation to the nucleus of spiral ganglion cells after the first cisplatin treatment cycle (day 5). These changes accompanied very modest increases in XPC and XPA mRNA levels in cochlear tissues which implies that transcriptional regulation is minimal compared to the nuclear translocation response of protein. The response kinetics of these enzymes provides a context for further interpreting these effects. Studies *in vitro* have shown that NER proteins such as XPC, XPA, ERCC1-XPF and TFIIH translocate rapidly to bind sites of UV damage to DNA, showing simple exponential kinetics with rate constant of 2 h and a similar residence time (Rademakers et al., 2003; Moné et al., 2004; Politi et al., 2005; Wu et al., 2007). These properties imply that nuclear binding of XPC and XPA at each time

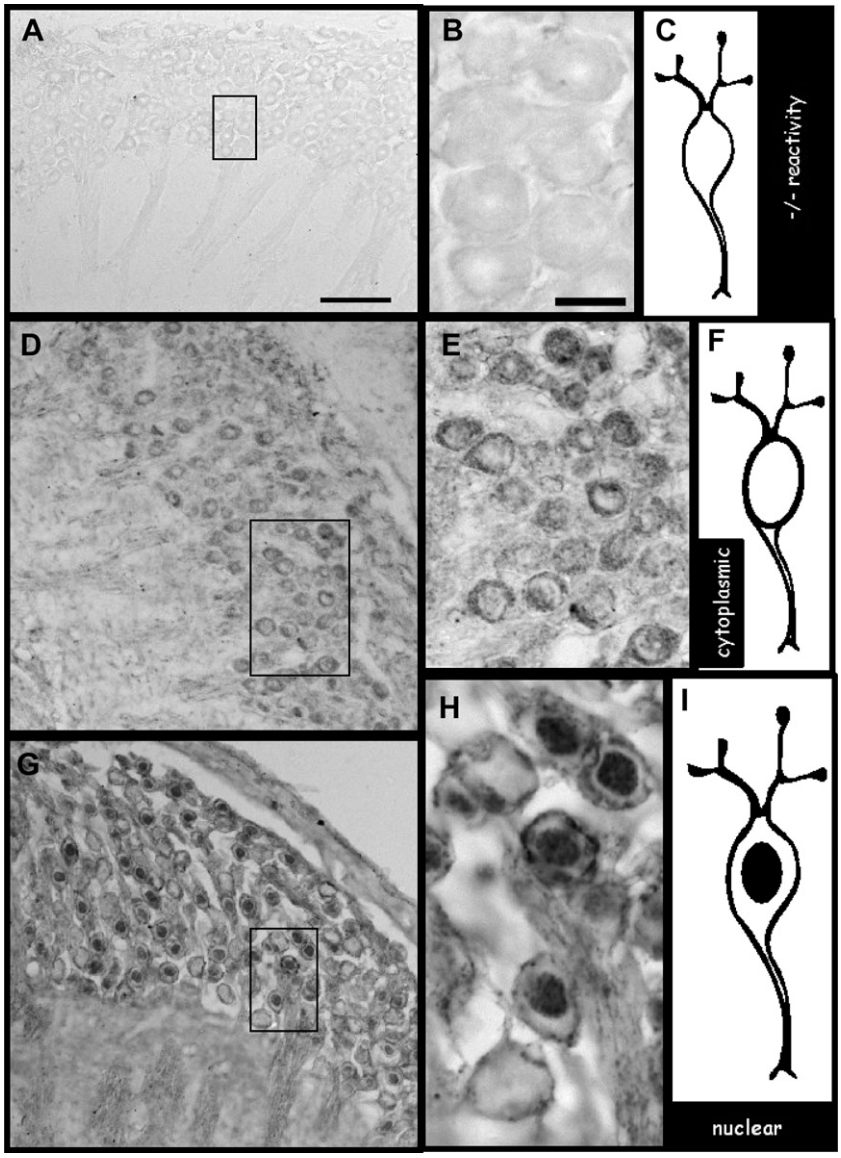

Fig. 3. Representative example of cytoplasmic to nuclear translocation among spiral ganglion neurons due to cisplatin treatment. (A) negative control showing no immunoreactivity. (B) The enlarged area in (A) showing cell bodies of spiral ganglion neurons. (C) A schematic representation of a bipolar spiral ganglion neuron from (A) with no immunoreactivity. (D) XPC immunoreactivity is present under normal conditions (saline treatment) among some spiral ganglion neurons. (E) The enlarged area outlined in (D) showing predominant cytoplasmic localization of XPC. (F) A schematic representation of a bipolar spiral ganglion neuron from (E) with prominent immunoreactivity in the cytoplasm. (G) XPC immunoreactivity remained present after cisplatin treatment among spiral ganglion cells, except the immunoreactivity is now predominantly localized in the nucleus (H), indicating translocation to the nucleus due to cisplatin treatment. (I) A schematic representation of a bipolar spiral ganglion neuron from (G) with prominent nuclear immunoreactivity. Scale bar (50 μm) in (A) applies to D and G as well. Scale bar (10 μm) in (B) applies to E and H as well.

point provide information about relatively instantaneous DNA NER activity within the affected cell populations.

The XPC response on day 5 is consistent with an ongoing activation of the GG-NER pathway which responds to DNA damage across the entire genome (Gillet and Schärer, 2006; Lainé and Egly, 2006). Because XPA activation is a downstream event for both GG-NER and TC-NER pathways (Lainé and Egly, 2006), the XPC and XPA nuclear staining pattern is consistent with activation of at least the GG-NER pathway by the first cycle of cisplatin exposure. However, the second cisplatin treatment cycle only resulted in an increased number of neurons with nuclear expression of XPA (day 19). Nuclear translocation of XPA and not XPC suggests that only the TC-NER pathway was activated on day 19. Four days after the conclusion of the second cisplatin treatment cycle (day 22) there was no significant difference in the proportion of ganglion cells with nuclear expression of either XPA or XPC, compared to saline controls. However, there was a significant increase in the proportion of cells expressing XPC in their cytoplasm, as well as a very modest increase in XPC mRNA in the treated cochleas.

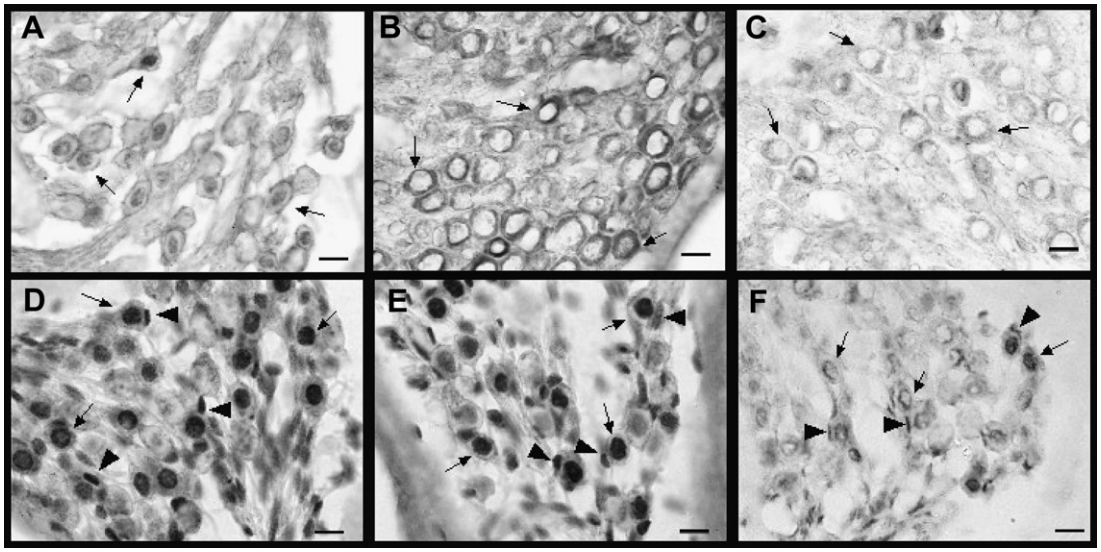

Fig. 4. Differential translocation of XPC (A–C) and XPA (D–F) among spiral ganglion neurons after cisplatin treatment. After the first treatment cycle (day 5) both XPC (A) and XPA (D) were localized in the nucleus of a proportion of spiral ganglion neurons (see arrows). After the second treatment cycle (day 19) XPA (E) remained localized in the nucleus while XPC (B) is now localized in the cytoplasm. After four days of recovery from the second treatment cycle (day 22) both XPC (C) and XPA (F) were predominantly localized in the cytoplasm. Interestingly, satellite cells (see arrow heads) were more immunnoreactive for XPA than for XPC and remained immunoreactive on all days sampled (D–F). Bars = 10 μm.

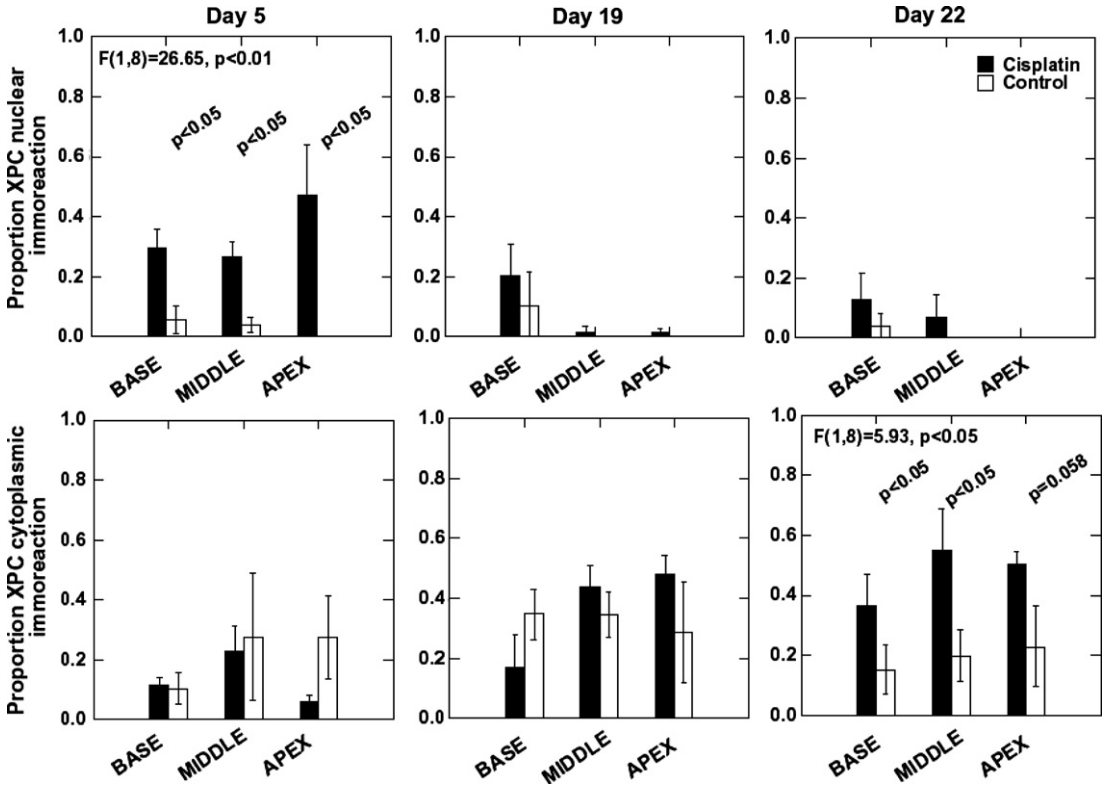

Fig. 5. Proportion of spiral ganglion neurons with either nuclear or cytoplamic XPC immunoreactivity as a function of cochlear turn. On day 5 a significant proportion of neurons exhibited nuclear localization of XPC compared to control. However, there was no significant difference in cytoplasmic expression between groups. On day 19 there was no significant change in nuclear localization of XPC from the control level. On day 22 there was no significant difference in nuclear localization between groups, but the proportion of cells with cytoplasmic XPC immunoreactivity was elevated significantly in the cisplatin treated group compared to control. These expression patterns suggest nuclear translocation of XPC after the first treatment cycle but increased cytoplasmic translation of XPC without nuclear translocation after the second treatment cycle. Each cochlear turn represents the mean ± SE of five animals from each treatment group.

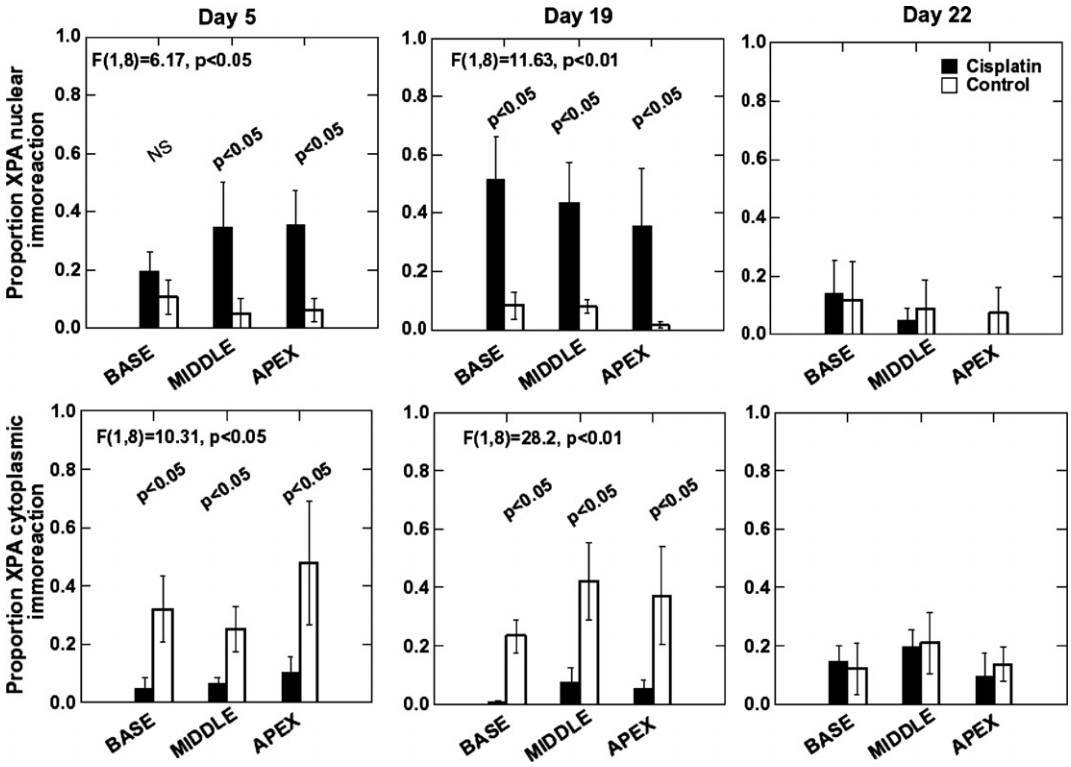

Fig. 6. Proportion of spiral ganglion neurons with either nuclear or cytoplasmic XPA immunoreactivity as a function of cochlear turn. On days 5 and 19 a significant proportion of spiral ganglion neurons exhibited high nuclear immunoreactivity accompanied by low cytoplasmic immunoreactivity after cisplatin treatment. Four days after the second cycle of treatment (day 22) there were no differences in immunoreactivity between groups. After the first treatment cycle (day 5), nuclear translocation was elevated significantly in the middle and apical cochlear turns but not in the basal turn. Significant nuclear translocation was observed in the basal turn after the second treatment cycle (day 19). Each cochlear turn represents the mean ± SE of the same five animals from each treatment group in Fig. 5.

The cytotoxic actions of cisplatin (*cis*-$\{(H_3N)_2Pt^{II}Cl_2\}$) likely reflect both formation of DNA adducts and binding to intracellular thiols such as glutathione (review: Siddik, 2003). The core of the cisplatin molecule and the site of reactivity is the metal ion platinum(II) which facilitates a *cis*-geometry between diammine $[(NH_3)_2]$ and dichloride (Cl_2) ligands. In cellular and extracellular milieu the Cl_2 ligand is subject to displacement reactions which convert the molecule to electrophilic species,

$$cis-\{(H_3N)_2Pt^{II}Cl_2\} + R_1 \rightarrow cis-\{(H_3N)_2Pt^{II}Cl_1\}^+ \quad (1)$$

$$cis-\{(H_3N)_2Pt^{II}Cl_1\}^+ + R_1 \rightarrow cis-\{(H_3N)_2Pt^{II}\}^{2+} \quad (2)$$

$$cis-\{(H_3N)_2Pt^{II}Cl_2\} + R_2 \rightarrow cis-\{(H_3N)_2Pt^{II}\}^{2+} \quad (3)$$

where R may be any of the following molecules, H_2O, $(H_2O)_2$, OH, $(OH)_2$, $(H_2O)(OH)$, NO, Br, I (Lippard, 1982). These electrophiles are significantly more reactive and ototoxic than the neutral parent compound and bind avidly to thiols such as GSH (Ekborn et al., 2000; Ishikawa and Ali-Osman, 1993). Cisplatin binds to GSH directly or enzymatically through GSH-*S*-transferase (GST) (Goto et al., 1999). Systemic cisplatin treatment has been shown to decrease cochlear GSH and GST levels while increasing ROS production (Ravi et al., 1995; Lautermann et al., 1997; Touliatos et al., 2000). Thus, one effect of cisplatin is increased ROS load in exposed cells by depleting antioxidant defenses. Depletion of antioxidant defenses may allow electrophilic platinum species to reach the nucleus and bind nucleophilic DNA sites.

The primary cytotoxic antineoplastic effect of cisplatin appears to be adduct formation in DNA (Fraval and Roberts, 1979; Reed et al., 1987). Cisplatin exhibits a high-affinity for the nucleophilic N7-sites of guanine residues of the DNA molecule and forms both monofunctional and bifunctional adducts (Eastman, 1986; Fichtinger-Schepman et al., 1987; Kelland, 2000). All cisplatin-DNA adducts may induce structural alterations to the DNA helix. The most common adducts are intrastrand N7–N7 links. Links between adjacent nucleotides are most prevalent, with 1,2-d(GpG) cross-links comprising up to 65% of all adducts and 1,2-d(ApG) links comprising about 25% of adducts; however, the intrastrand 1,3-d(GpNpG) adducts (with one nucleotide separating linked guanines) also comprise 5–10% of the lesions (review: Gillet and Schärer, 2006). The dominant 1,2-d(GpG) intrastrand cisplatin adduct between adjacent nucleotides appear to be relatively refractory to NER (e.g. Szymkowski et al., 1992), but the interstrand adducts separated by a nucleotide are repaired more readily. The observed nuclear translocation of XPC and XPA is likely to reflect adduct repair

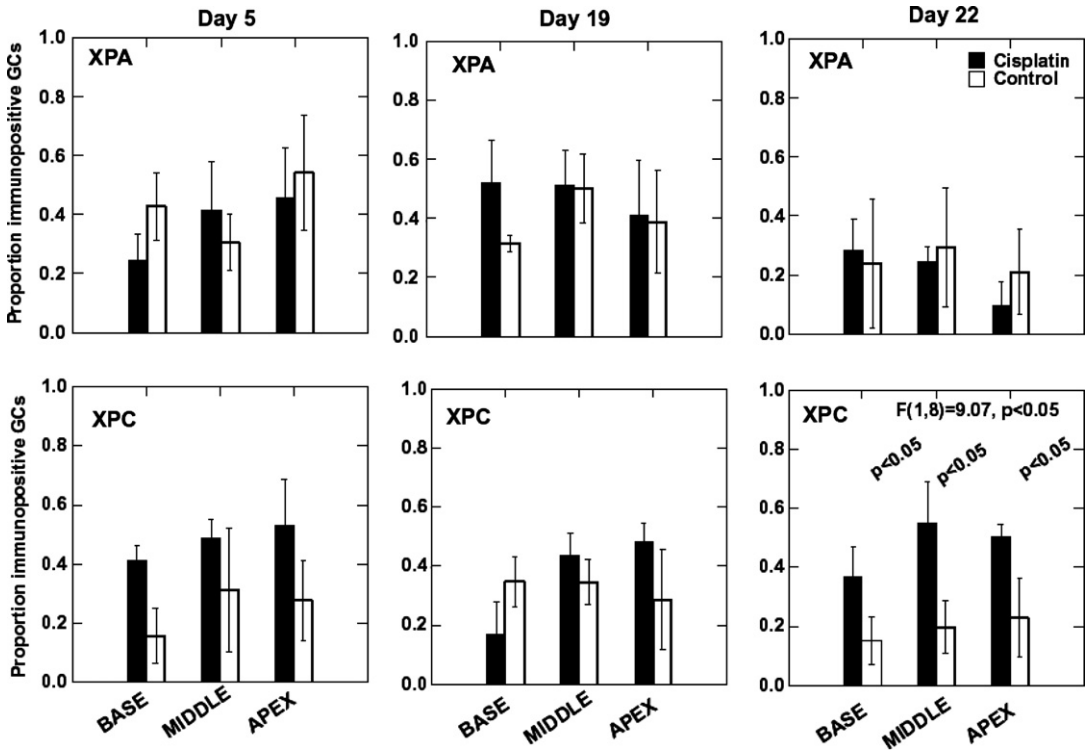

Fig. 7. The total proportion of spiral ganglion neurons that are immunoreactive for XPC and XPA regardless of nuclear or cyoplasmic immunoreactivity. Note that a similar proportion of neurons that are immunoreactive under normal conditions are also immunoreactive after cisplatin treatment. Each cochlear turn represents the mean ± SE of the same five animals from each treatment group in Figs. 5 and 6.

Table 3
Results of analysis of variance of immunohistochemical analyses of XPC distribution

Source	df	*F*-values					
		Apex		Middle		Base	
		Nuclear	Cytoplasmic	Nuclear	Cytoplasmic	Nuclear	Cytoplasmic
Days (*D*)	2	9.610[a]	3.047	9.760[a]	0.986	0.941	2.815
Treatment (*T*)	1	10.521[a]	1.093	13.459[a]	2.170	5.990[b]	0.080
$D \times T$	2	9.675[a]	3.696[b]	5.170[b]	1.750	0.717	3.744[b]
MS_{Error}	24	0.018	0.046	0.006	0.059	0.025	0.026

The *F*-ratios are shown for separate two-way analyses of the proportion of nuclear immunoreactive and cytoplasmic immunoreactive spiral ganglion cells from different sites in the cochlea. Significant main effects for days (day 5, 19 and 22) and treatment (saline and cisplatin) and the significant days × treatment interactions are indicated.

[a] $p < .01$.
[b] $p < .05$.

Table 4
Results of analysis of variance of immunohistochemical analyses of XPA distribution

Source	df	*F*-values					
		Apex		Middle		Base	
		Nuclear	Cytoplasmic	Nuclear	Cytoplasmic	Nuclear	Cytoplasmic
Days (*D*)	2	2.186	1.357	2.648	0.740	2.178	0.645
Treatment (*T*)	1	6.538[b]	8.069[a]	8.740[a]	9.459[a]	6.244[b]	10.609[a]
$D \times T$	2	3.256	1.430	3.119	2.632	3.113	3.595[b]
MS_{Error}	24	0.040	0.056	0.036	0.027	0.040	0.018

The *F*-ratios are shown for separate two-way analyses of the proportion of nuclear immunoreactive and cytoplasmic immunoreactive spiral ganglion cells from different sites in the cochlea. Significant main effects for days (day 5, 19 and 22) and treatment (saline and cisplatin) and the significant days × treatment interactions are indicated.

[a] $p < .01$.
[b] $p < .05$.

because cisplatin adducts have been reported in all cochlear tissues after systemic treatment (Thomas et al., 2006; van Ruijven et al., 2005).

Recent evidence suggests that NER mechanisms may also be important for repair of some forms of oxidative DNA damage (Brooks et al., 2000; Kuraoka et al., 2000; D'Errico et al., 2006). Activation of XPA appears to be important for repair of one class of ROS-induced DNA lesion, 5′,8-purine cyclodeoxynucleosides (Brooks et al., 2000; Kuraoka et al., 2000). Recent studies in XPC-deficient cells suggest that XPC may be a cofactor in excision repair of 8-OH-guanine lesions in DNA (D'Errico et al., 2006). However, XPA and XPC are only one of a number of substrates for repairing oxidative lesions to DNA, which include long patch and short patch base excision repair pathways and mismatch repair pathways (Slupphaug et al., 2003). The former pathway appears to be the primary mechanism for repairing oxidative damage.

The sequence of NER responses suggests an evolving process of DNA damage in the spiral ganglion across the cycles of cisplatin exposure. During the first treatment cycle, cisplatin binding to DNA may be limited by extensive cisplatin binding to cytoplasmic thiols (such as glutathione), which constitutes a detoxification mechanism (e.g. Siddik, 2003). Hence, the XPC and XPA translocation to the nucleus of spiral ganglion cells on day 5 is likely to be a GG-NER (and possibly, TC-NER) response to manage low levels of genomic DNA damage. The translocation of only XPA after the second cycle of exposure (day 19) may reflect a primary TC-NER response to increased DNA exposure to cisplatin, both as a secondary consequence of thiol (e.g. glutathione) depletion and an associated increase in vulnerability to oxidative DNA damage.

One interesting feature of the NER response was the lack of a significant XPA translocation among basal spiral ganglion neurons on day 5, despite a robust XPC translocation. This finding contrasted with the robust XPA translocation in middle and apical spiral ganglion neurons. Human temporal bone histopathological studies indicate that apical spiral ganglion neurons are less vulnerable to cisplatin damage than neurons at the cochlear base (Cheng et al., 2001; Hoistad et al., 1998; Strauss et al., 1983). It is tempting to suggest that a decreased early mobilization of XPA translocation in basal turn spiral ganglion neurons may contribute to this increased susceptibility to injury.

Acknowledgements

The authors would like to thank Drs. Catherine Palmer and Sheila Pratt for helpful discussions and Chia-Yi Lo and Gloria Limetti for expert technical assistance. This work was supported by NIH-NIDCD (F31 DC05757-03), the K. Leroy Irvis Award and the SHRS Research Development Fund, all awarded to OWG and the Eye and Ear Institute Foundation (CDB).

References

Boonstra, A., van Oudenaren, A., Baert, M., van Steeg, H., Leenen, P.J.M., van der Horst, G.T.J., Hoeijmakers, J.H.J., Savelkoul, H.F.J., Garssen, J., 2001. Differential ultraviolet-B-induced immunomodulation in XPA, XPC, and CSD DNA repair-deficient mice. J. Invest. Dermatol. 117, 141–146.

Brooks, P.J., Wise, D.S., Berry, D.A., Kosmoski, J.V., Smerdon, M.J., Somers, R.L., Mackie, H., Spoonde, A.Y., Ackerman, E.J., Coleman, K., Tarone, R.E., Robbins, J.H., 2000. The oxidative DNA lesion 8,5′-(S)-cyclo-2′-deoxyadenosine is repaired by the nucleotide excision repair pathway and blocks gene expression in mammalian cells. J. Biol Chem. 275, 22355–22362.

Cheng, P.-W., Kaga, K., Koyama, S., Kondo, K., 2001. Temporal bone histopathology after treatment by a large amount of cisplatin: a case study. Otolaryngol. Head Neck Surg. 125, 411–413.

Chen, Z., Xu, X.S., Yang, J., Wang, G., 2003. Defining the function of XPC protein in psoralen and cisplatin-mediated DNA repair and mutagenesis. Carcinogenesis 24, 1111–1121.

Clerici, W.J., Hensley, K., DiMartino, D.L., Butterfield, D.A., 1996. Direct detection of ototoxicant-induced reactive oxygen species generation in cochlear explants. Hear. Res. 8, 116–124.

Costa, R.M.A., Chigancas, V., Galhardo, R.D.S., Carvalho, H., Menck, C.F.M., 2003. The eukaryotic nucleotide excision repair pathway. Biochimie 85, 1083–1099.

Dabholkar, M., Vionnet, J., Bostick-Bruton, F., Yu, J.J., Reed, E., 1994. Messenger RNA levels of XPAC and ERCC1 in ovarian cancer tissue correlate with response to platinum-based chemotherapy. J. Clin. Invest. 94, 703–708.

de Laat, W.L., Jaspers, N.G.J., Hoeijmakers, J.H.J., 1999. Molecular mechanism of nucleotide excision repair. Gene. Dev. 13, 768–785.

D'Errico, M., Parlanti, E., Teson, M., de Jesus, B.M., Degan, P., Calcagnile, A., Jaruga, P., Bjørås, M., Crescenzi, M., Pedrini, A.M., Egly, J.M., Zambruno, G., Stefanini, M., Dizdaroglu, M., Dogliotti, E., 2006. New functions of XPC in the protection of skin cells from oxidative damage. EMBO J. 25, 4305–4315.

Eastman, A., 1986. Reevaluation of interaction of cis-dichloro(ethylenediamine)platinum(II) with DNA. Biochemistry 25, 3912–3915.

Ekborn, A., Laurell, G., Andersson, A., Wallin, I., Eksborg, S., Ehrsson, H., 2000. Cisplatin-induced hearing loss: Influence of mode of drug administration in the guinea pig. Hear. Res. 140, 38–44.

Ferry, K.V., Hamilton, T.C., Johnson, S.W., 2000. Increased nucleotide excision repair in cisplatin resistant ovarian cancer cells. Biochem. Pharmacol. 60, 1305–1313.

Fichtinger-Schepman, A.M., van Oosterom, A.T., Lohman, P.H., Berends, F., 1987. *cis*-Diamminedichloroplatinum(II)-induced DNA adducts in peripheral leukocytes from seven cancer patients: Quantitative immunochemical detection of the adduct induction and removal after a single dose of *cis*-diamminedichloroplatinum(II). Cancer Res. 47, 3000–3004.

Fraval, H.N., Roberts, J.J., 1979. Excision repair of *cis*-diamminedichloroplatinum(II)-induced damage to DNA of Chinese hamster cells. Cancer Res. 39, 1793–1797.

Giaccone, G., 2000. Clinical perspectives on platinum resistance. Drugs 59 (Suppl. 4), 9–17.

Gillet, L.C.J., Schärer, O.D., 2006. Molecular mechanisms of mammalian global excision repair. Chem. Rev. 106, 253–276.

Goto, S., Iida, T., Cho, S., Oka, M., Kohno, S., Kondo, T., 1999. Overexpression of glutathione *S*-transferase pi enhances the adduct formation of cisplatin with glutathione in human cancer cells. Free Radical Res. 31, 549–558.

Hoistad, D.L., Ondrey, F.G., Mutlu, C., Schachern, P.A., Paparella, M.M., Adams, G.L., 1998. Histopathology of human temporal bone after *cis*-platinum, radiation, or both. Otolaryngol. Head Neck Surg. 118, 825–832.

Ishikawa, T., Ali-Osman, F., 1993. Glutathione-associated *cis*-diamminedichloroplatinum(II) metabolism and ATP-dependent efflux from

leukemia cells: molecular characterization of glutathione–platinum complex and its biological significance. J. Biol. Chem. 268, 20116–20125.

Kartalou, M., Essigmann, J.M., 2001. Recognition of cisplatin adducts by cellular proteins. Mutat. Res. 478, 1–21.

Kelland, L.R., 2000. Preclinical perspectives on platinum resistance. Drugs 59 (Suppl. 4), 1–8.

Koberle, B., Masters, J.R.W., Hartkey, J.A., Wood, R.D., 1999. Defective repair of cisplatin-induced DNA damage caused by reduced XPA protein in testicular germ cell tumours. Curr. Biol. 9, 273–276.

Kuraoka, I., Bender, C., Romieu, A., Cadet, J., Wood, R.D., Lindahl, T., 2000. Removal of oxygen free-radical-induced 5′,8-purine cyclodeoxynucleosides from DNA by the nucleotide excision-repair pathway in human cells. Proc. Natl. Acad. Sci. USA 97, 3832–3837.

Lainé, J.-P., Egly, J.-M., 2006. When transcription and repair meet: a complex system. Trends Genet. 22, 430–436.

Lautermann, J., Crann, S.A., McLaren, J., Schacht, J., 1997. Glutathione-dependent antioxidant systems in mammalian inner ear: effects of aging, ototoxicity drugs and noise. Hear. Res. 114, 75–82.

Lippard, S.J., 1982. New chemistry of an old molecule: *cis*-$(Pt(NH_3)_2Cl_2$. Science 218, 1075–1082.

Livak, K.J., Schmittgen, T.D., 2001. Analysis of relative gene expression data using real time quantitative PCR and the $2^{-\Delta\Delta CT}$ method. Methods. 25, 402–408.

McLean, I.W., Nakane, P.K., 1974. Periodate–lysine–paraformaldehyde fixative for immunoelectron microscopy. J. Histochem. Cytochem. 22, 1077–1083.

Minami, S.B., Sha, S.-H., Schacht, J., 2004. Antioxidant protection in a new animal model of cisplatin-induced ototoxicity. Hear. Res. 198, 137–143.

Moné, M.J., Bernas, T., Dinant, C., Goedvree, F.A., Manders, E.M.M., Volker, M., Houtsmuller, A.B., Hoeijmakers, J.H.J., Vermeulen, W., van Driel, R., 2004. In vivo dynamics of chromatin-associated complex formation in mammalian nucleotide excision repair. PNAS 101, 15933–15937.

Pera, M.F., Rawlings, C.J., Roberts, J.J., 1981. The role of DNA repair in the recovery of human cells from cisplatin toxicity. Chem. Biol. Interact. 37, 245–261.

Politi, A., Moné, M.J., Houtsmuller, A.B., Hoogstraten, D., Vermeulen, W., Heinrich, R., van Driel, R., 2005. Mathematical modeling of nucleotide excision repair reveals efficiency of sequential assembly strategies. Mol. Cell 19, 679–690.

Rademakers, S., Volker, M., Hoogstraten, D., Nigg, A.L., Moné, M.J., van Zeeland, A.A., Hoeijmakers, J.H.J., Houtsmuller, A.B.D., Vermeulen, W., 2003. Xeroderma pigmentosum group A protein loads as a separate factor onto DNA lesions. Mol. Cellular Biol. 23, 5755–5767.

Ravi, R., Somani, S.M., Rybak, L.P., 1995. Mechanism of cisplatin ototoxicity: antioxidant system. Pharmacol. Toxicol. 76, 386–396.

Reed, E., Ozols, R.F., Tarone, R., Yuspa, S.H., Poirier, M.C., 1987. Platinum-DNA adducts in leukocyte DNA correlate with disease response in ovarian cancer patients receiving platinum-based chemotherapy. Proc. Natl. Acad. Sci. USA 84, 5024–5028.

Redon, S., Bombard, S., Elizondo-Riojas, M.A., Chottard, J.C., 2003. Platinum cross-linking of adenines and guanines on the quadruplex structures of the AG3(T2AG3)3 and (T2AG3)4 human telomere sequences in Na^+ and K^+ solutions. Nucleic Acids Res. 31, 1605–1613.

Riedl, T., Hanaoka, F., Egly, J.-M., 2003. The coming and goings of nucleotide excision repair factors on damaged DNA. EMBO J. 22, 5293–5303.

Rosenberg, E., Taher, M.M., Kuemmerle, N.B., Farnsworth, J., Valerie, K., 2001. A truncated human xeroderma pigmentosum complementation group A protein expressed from an adenovirus sensitizes human tumor cells to ultraviolet light and cisplatin. Cancer Res. 61, 764–770.

Schmittgen, T.D., Zakrajsek, B.A., Mills, A.G., Gorn, V., Singer, M.J., Reed, M.W., 2000. Quantitative reverse transcription-polymerase chain reaction to study mRNA decay: comparison of endpoint and real-time methods. Anal. Biochem. 285, 194–204.

Selvakumaran, M., Pisarcik, D.A., Bao, R., Yeung, A.T., Hamilton, T.C., 2003. Enhanced cisplatin cytotoxicity by disturbing the nucleotide excision repair pathway in ovarian cancer cell lines. Cancer Res. 63, 1311–1316.

Siddik, Z.H., 2003. Cisplatin: mode of cytotoxic action and molecular basis of resistance. Oncogene 22, 7265–7279.

Slupphaug, G., Kavli, B., Krokan, H.E., 2003. The interacting pathways for prevention and repair of oxidative DNA damage. Mutat. Res. 531, 231–251.

Strauss, M., Towfighi, J., Lord, S., Lipton, A., Harvey, H.A., Brown, B., 1983. Cis-platin ototoxicity: clinical experience and temporal bone histopathology. Laryngoscope 93, 1554–1559.

Szymkowski, D.E., Yarema, K., Essigmann, J.M., Lippard, S.J., Wood, R.D., 1992. An intrastrand d(GpG) platinum crosslink in duplex M13 DNA is refractory to repair by human cell extracts. Proc. Natl. Acad. Sci. USA 89, 10772–10776.

Thoma, B.S., Vasquez, K.M., 2003. Critical DNA damage recognition functions of XPC-hHR23B and XPA-RPA in nucleotide excision repair. Mol. Carcinogen. 38, 1–13.

Thomas, J.P., Lautermann, J., Liedert, B., Seiler, F., Thomale, J., 2006. High accumulation of platinum-DNA adducts in strial marginal cells of the cochlea is an early event in cisplatin but not carboplatin ototoxicity. Mol. Pharmacol. 70, 23–29.

Tornaletti, S., Patrick, S.M., Turchi, J.J., Hanawalt, P.C., 2003. Behavior of T7 RNA polymerase and mammalian RNA polymerase II at site-specific cisplatin adducts in the template DNA. J. Biol. Chem. 278, 35791–35797.

Touliatos, J.S., Neitzel, L., Whitworth, C., Rybak, L.P., Malafa, M., 2000. Effect of cisplatin on the expression of glutathione-*S*-transferase in the cochlea of the rat. Eur. Arch. Otorhinolaryngol. 257, 6–9.

van Ruijven, M.W.M., de Groot, J.C.M.J., Hendriksen, F., Smoorenburg, G.F., 2005. Immunohistochemical detection of platinated DNA in the cochlea of cisplatin-treated guinea pigs. Hear. Res. 203, 112–121.

Welsh, C., Day, R., McGurk, C., Masters, J.R., Wood, R.D., Koberle, B., 2004. Reduced levels of XPA, ERCC1 and XPF DNA repair proteins in testis tumor cell lines. Int. J. Cancer 110, 352–361.

Wu, X., Fan, W., Xu, S., Zhou, Y., 2003. Sensitization to the cytotoxicity of cisplatin by transfection with nucleotide excision repair gene xeroderma pigmentosum group A antisense RNA in human lung adenocarcinoma cells. Clin. Cancer Res. 9, 5874–5879.

Wu, X., Shell, S.M., Liu, Y., Zou, Y., 2007. ATR-dependent checkpoint modulates XPA nuclear import in response to UV irradiation. Oncogene 26, 757–764.

Zastawny, T.H., Olejniczak, W., Olinski, R., 1993. Cis-DDP induced alteration of DNA structure studied by scanning tunneling microscopy. Acta Biochim. Pol. 40, 555–558.